

AD-A137 129

COUPLING BETWEEN TWO ARBITRARILY ORIENTED DIPOLES
THROUGH MULTILAYERED SHIELDS(U) ILLINOIS UNIV AT URBANA
ELECTROMAGNETICS LAB R YANG ET AL. JUN 83 UIEM-83-7
N00014-81-K-0245

1/1

UNCLASSIFIED

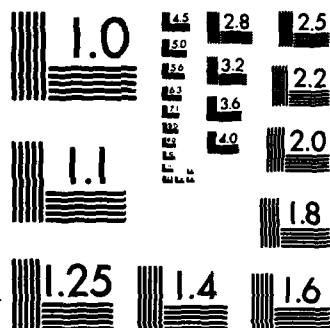
F/G 20/3

NL

END

FILED

DTIC



MICROCOPY RESOLUTION TEST CHART
NATIONAL BUREAU OF STANDARDS-1963-A

DTIC
ELECTROMAGNETICS LABORATORY
TECHNICAL REPORT NO. 83-7

June 1983

AD A137129

COUPLING BETWEEN TWO ARBITRARILY ORIENTED
DIPOLES THROUGH MULTILAYERED SHIELDS

R. YANG

R. MITTRA



THE PHYSICS DEPARTMENT
TECHNICAL REPORT NO. 83-7
JAN 23 1984
NAVAL RESEARCH LABORATORY

DTIC FILE COPY

This document has been approved
for public release and sale; its
distribution is unlimited.

DTIC
ELECTE
JAN 23 1984
JFA

ELECTROMAGNETICS LABORATORY
DEPARTMENT OF ELECTRICAL ENGINEERING
ENGINEERING EXPERIMENT STATION
UNIVERSITY OF ILLINOIS AT URBANA-CHAMPAIGN
URBANA, ILLINOIS 61801

SUPPORTED BY
CONTRACT NO. N00014-81-K-0245
PHYSICAL SCIENCES DIVISION
OFFICE OF NAVAL RESEARCH
DEPARTMENT OF THE NAVY
ARLINGTON, VIRGINIA 22217

84 01 23 05

SECURITY CLASSIFICATION OF THIS PAGE (When Data Entered)

REPORT DOCUMENTATION PAGE		READ INSTRUCTIONS BEFORE COMPLETING FORM
1. REPORT NUMBER	2. GOVT ACCESSION NO.	3. RECIPIENT'S CATALOG NUMBER
4. TITLE (and Subtitle) COUPLING BETWEEN TWO ARBITRARILY ORIENTED DIPOLES THROUGH MULTILAYERED SHIELDS		5. TYPE OF REPORT & PERIOD COVERED Technical
		6. PERFORMING ORG. REPORT NUMBER EM 83-7; UILU-ENG-83-2546
7. AUTHOR(s) R. Yang and R. Mittra		8. CONTRACT OR GRANT NUMBER(s) N00014-81-K-0245
9. PERFORMING ORGANIZATION NAME AND ADDRESS Electromagnetics Laboratory Department of Electrical Engineering University of Illinois, Urbana, Illinois 61801		10. PROGRAM ELEMENT, PROJECT, TASK AREA & WORK UNIT NUMBERS Project No. 410
11. CONTROLLING OFFICE NAME AND ADDRESS Office of Naval Research Department of the Navy Arlington, Virginia 22217		12. REPORT DATE June 1983
		13. NUMBER OF PAGES 40
14. MONITORING AGENCY NAME & ADDRESS (if different from Controlling Office)		15. SECURITY CLASS. (of this report) Unclassified
		15a. DECLASSIFICATION/DOWNGRADING SCHEDULE
16. DISTRIBUTION STATEMENT (of this Report) Distribution Unlimited		
17. DISTRIBUTION STATEMENT (of the abstract entered in Block 20, if different from Report)		
18. SUPPLEMENTARY NOTES		
19. KEY WORDS (Continue on reverse side if necessary and identify by block number) Multilayered Shields; Plane-Wave Spectral Representation; Coupling; Arbitrarily Oriented Dipoles; Transformed Matrices		
20. ABSTRACT (Continue on reverse side if necessary and identify by block number) An analysis of the electromagnetic coupling between two arbitrarily oriented dipoles through planar multilayered shields is made. This method of approach is based on the plane-wave spectral representation of radiation fields and the use of transformation matrices for multilayered media. Numerical results are found to be in good agreement with the experimental data obtained in the frequency range from 10 kHz to 1 MHz.		

Electromagnetics Laboratory Report No. 83-7

COUPLING BETWEEN TWO ARBITRARILY ORIENTED DIPOLES THROUGH MULTILAYERED SHIELDS

by

R. Yang*
R. Mittra

Electromagnetics Laboratory
Department of Electrical Engineering
University of Illinois at Urbana-Champaign
Urbana, Illinois 61801

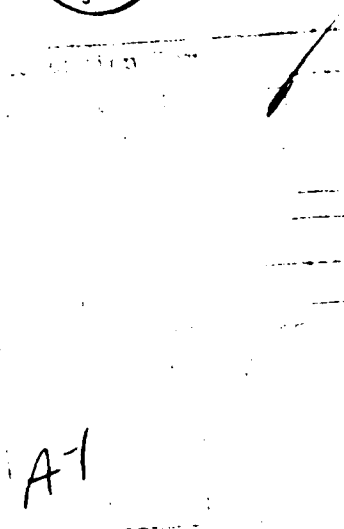
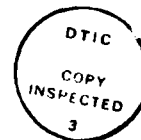
*On leave from
Xian Jiaolong University
Xian, Shaanxi Province
The People's Republic of China

Technical Report

June 1983

Supported by

Contract No. N00014-81-K-0245
Physical Sciences Division
Office of Naval Research
Department of the Navy
Arlington, Virginia 22217



ABSTRACT

An analysis of the electromagnetic coupling between two arbitrarily oriented dipoles through planar multilayered shields is made. This method of approach is based on the plane-wave spectral representation of radiation fields [1] and the use of transformation matrices for multilayered media. Numerical results are found to be in good agreement with the experimental data obtained in the frequency range from 10 kHz to 1 MHz.

TABLE OF CONTENTS

	Page
1. INTRODUCTION.	1
2. TRANSFORMATION MATRIX [T] FOR PLANE WAVES	2
3. SPECTRAL REPRESENTATION OF THE RADIATION FIELDS	11
4. NUMERICAL COMPUTATION	15
4.1. Collinear Magnetic Dipoles (or Small Coaxial Loops)	15
4.2. Collinear Electric Dipole	22
5. NUMERICAL RESULTS	25
6. CONCLUSION.	28
APPENDIX 1: FIELD EQUATIONS.	29
APPENDIX 2: COORDINATE TRANSFORMATION.	32
REFERENCES.	35

LIST OF FIGURES

Figure		Page
1.	The geometry of propagation of the perpendicular (a) and parallel (b) components.	3
2.	Multilayered media	9
3.	Two coaxial loops separated by a shield.	16
4.	Contour transformation	20
5.	Two coaxial loops separated by a double copper shield.	23
6.	Theoretical and experimental results for electric dipoles, plane wave and magnetic dipoles.	26
7.	The propagation direction of each of the components radiated by the dipole.	27
A.1.	Contour for $z > z'$	31
A.2.	Contour for $z < z'$	31
A.3.	Coordinate transformation.	33

1. INTRODUCTION

It is well-known that an arbitrary field can be represented in terms of its plane-wave spectral representation. In this paper, we employ this representation to express the incident and scattered fields from multilayered media as follows

$$E(x,y,z) = \iint \tilde{E}(\alpha,\beta) e^{j(\alpha x + \beta y + \gamma z)} d\alpha d\beta \quad (1)$$

$$H(x,y,z) = \iint \tilde{H}(\alpha,\beta) e^{j(\alpha x + \beta y + \gamma z)} d\alpha d\beta \quad (2)$$

where $\gamma = \sqrt{k^2 - \alpha^2 - \beta^2}$, $k = \omega\sqrt{\mu\epsilon}$ and \sim on top indicates Fourier transform. For a plane wave that is incident on the boundary between two media from an arbitrary direction, it is possible to find a matrix relationship between the fields in the two regions separated by the boundary. The matrix may be termed the transformation matrix and will be very useful for our analysis. In order to simplify the representation of the transformation matrix, it is useful to resolve the incident wave into two components, one parallel to the plane of incidence, and the other perpendicular to the same. These two components will be denoted by subscripts (\parallel - parallel, \perp - perpendicular), propagate independently, and remain uncoupled throughout the processes of reflection and transmission at the interface between dissimilar media. Hence, the transformation matrix for the fields expressed in terms of the parallel and perpendicular components (to the plane of incidence) becomes diagonal.

2. TRANSFORMATION MATRIX [T] FOR PLANE WAVES

In this section, we first derive the transformation matrix for a single interface between two dissimilar media. The extension to the multilayered case is considered later. Let us define two reference planes that are parallel to the boundary at $Z = 0$, namely, plane 1 and plane 2, as shown in Fig. 1. The waves $E_{\perp}^{1\oplus}$ and $E_{\perp}^{1\ominus}$ are at plane 1, and $E_{\perp}^{2\oplus}$ and $E_{\perp}^{2\ominus}$ are at plane 2. The \oplus sign indicates waves propagating in the $+z$ -direction, whereas the \ominus sign indicates waves propagating in the opposite direction.

Next we resolve the incident electric field of the incident wave into the parallel and perpendicular components. Figures 1a and 1b illustrate the geometry of propagation of the perpendicular and parallel components, respectively. The boundary condition that must be satisfied on the interface between the two dissimilar media is that the tangential components of the fields E and H be continuous. Enforcing these conditions we get

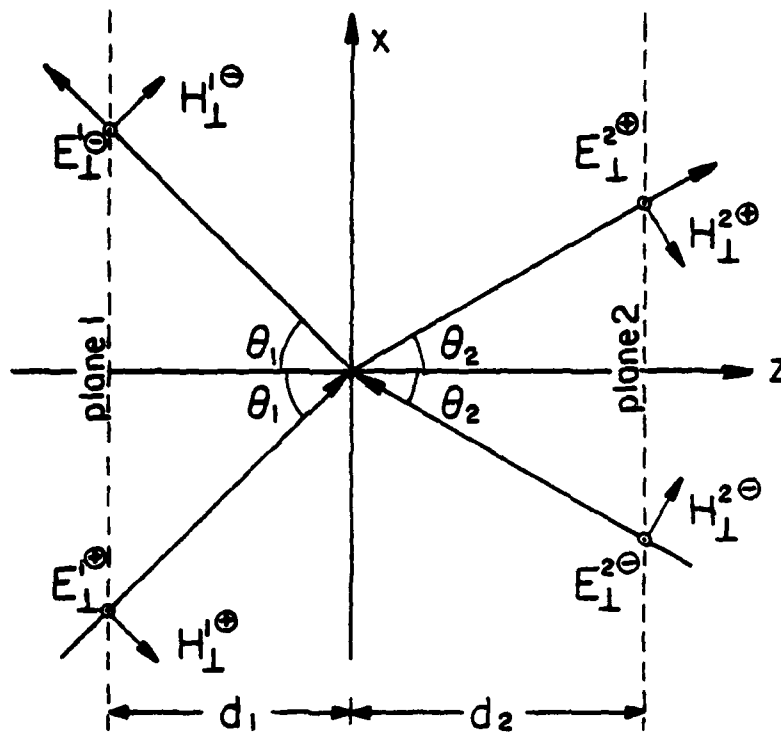
$$E_{\perp}^{1\oplus} e^{jr_1 d_1} + E_{\perp}^{1\ominus} e^{-jr_1 d_1} = E_{\perp}^{2\oplus} e^{-jr_2 d_2} + E_{\perp}^{2\ominus} e^{jr_2 d_2} \quad (3)$$

$$-H_{\perp}^{1\oplus} e^{jr_1 d_1} \cos \theta_1 + H_{\perp}^{1\ominus} e^{-jr_1 d_1} \cos \theta_1 = H_{\perp}^{2\oplus} e^{-jr_2 d_2} \cos \theta_2 + H_{\perp}^{2\ominus} e^{jr_2 d_2} \cos \theta_2 \quad (4)$$

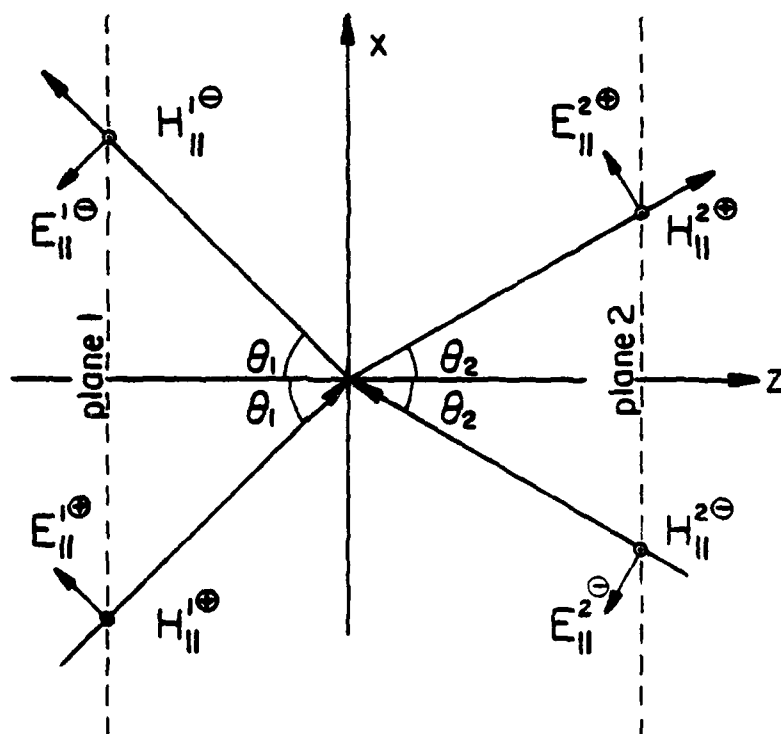
where d_1 and d_2 are distances of the terminal planes from the interface, and θ_1 and θ_2 are the angles between the directions of propagation and the normals of the interface, as shown in Fig. 1. Therefore, we have

$$\cos \theta_1 = \frac{\bar{k}_1 \cdot \hat{z}}{|\bar{k}_1|} = \frac{\sqrt{k_1^2 - \alpha^2 - \beta^2}}{|\bar{k}_1|} \quad (5)$$

$$\cos \theta_2 = \frac{\bar{k}_2 \cdot \hat{z}}{|\bar{k}_2|} = \frac{\sqrt{k_2^2 - \alpha^2 - \beta^2}}{|\bar{k}_2|} \quad (6)$$



(a)



(b)

Figure 1. The geometry of propagation of the perpendicular (a) and parallel (b) components.

Note that the phase factor e^{jkr} is assumed here. Rewriting Eq. (4) and using $H = \sqrt{\epsilon/\mu} E$, we obtain

$$\sqrt{\frac{\epsilon_1}{\mu_1}} (E_1^{1\oplus} e^{jr_1 d_1} - E_1^{1\ominus} e^{-jr_1 d_1}) \cos \theta_1 = \sqrt{\frac{\epsilon_2}{\mu_2}} (E_1^{2\oplus} e^{-jr_2 d_2} - E_1^{2\ominus} e^{jr_2 d_2}) \cos \theta_2 \quad (7)$$

Multiplying Eq. (3) by $(\sqrt{\epsilon_1/\mu_1} \cos \theta_1)$ and subtracting from Eq. (7), we have

$$2E_1^{1\oplus} e^{-jr_1 d_1} \sqrt{\frac{\epsilon_1}{\mu_1}} \cos \theta_1 = E_1^{2\oplus} e^{-jr_2 d_2} \left(\sqrt{\frac{\epsilon_1}{\mu_1}} \cos \theta_1 + \sqrt{\frac{\epsilon_2}{\mu_2}} \cos \theta_2 \right) + E_1^{2\ominus} e^{-jr_2 d_2} \left(\sqrt{\frac{\epsilon_1}{\mu_1}} \cos \theta_1 - \sqrt{\frac{\epsilon_2}{\mu_2}} \cos \theta_2 \right) \quad (8)$$

Similarly, multiplying Eq. (3) by $(\sqrt{\epsilon_1/\mu_1} \cos \theta_1)$ and subtracting from Eq. (7), we have

$$2E_1^{1\ominus} e^{-jr_1 d_1} \sqrt{\frac{\epsilon_1}{\mu_1}} \cos \theta_1 = E_1^{2\oplus} e^{-jr_2 d_2} \left(\sqrt{\frac{\epsilon_1}{\mu_1}} \cos \theta_1 - \sqrt{\frac{\epsilon_2}{\mu_2}} \cos \theta_2 \right) + E_1^{2\ominus} e^{-jr_2 d_2} \left(\sqrt{\frac{\epsilon_1}{\mu_1}} \cos \theta_1 + \sqrt{\frac{\epsilon_2}{\mu_2}} \cos \theta_2 \right) \quad (9)$$

From Eqs. (8) and (9), we obtain

$$\begin{bmatrix} E_1^{1\oplus} \\ E_1^{1\ominus} \end{bmatrix} = [T] \begin{bmatrix} E_1^{2\oplus} \\ E_1^{2\ominus} \end{bmatrix} \quad (10)$$

where

$$[T]_{\perp}^E = \begin{bmatrix} \frac{\sqrt{\frac{\epsilon_1}{\mu_1}} \cos \theta_1 + \sqrt{\frac{\epsilon_2}{\mu_2}} \cos \theta_2}{2 \sqrt{\frac{\epsilon_1}{\mu_1}} \cos \theta_1} e^{-j r_2 d_2 - j r_1 d_1}, & \frac{\sqrt{\frac{\epsilon_1}{\mu_1}} \cos \theta_1 - \sqrt{\frac{\epsilon_2}{\mu_2}} \cos \theta_2}{2 \sqrt{\frac{\epsilon_1}{\mu_1}} \cos \theta_1} e^{j r_2 d_2 - j r_1 d_1} \\ \frac{\sqrt{\frac{\epsilon_1}{\mu_1}} \cos \theta_1 - \sqrt{\frac{\epsilon_2}{\mu_2}} \cos \theta_2}{2 \sqrt{\frac{\epsilon_1}{\mu_1}} \cos \theta_1} e^{-j r_2 d_2 + j r_1 d_1}, & \frac{\sqrt{\frac{\epsilon_1}{\mu_1}} \cos \theta_1 + \sqrt{\frac{\epsilon_2}{\mu_2}} \cos \theta_2}{2 \sqrt{\frac{\epsilon_1}{\mu_1}} \cos \theta_1} e^{j r_2 d_2 + j r_1 d_1} \end{bmatrix} \quad (11)$$

The matrix $[T]_{\perp}^E$ is termed a transformation matrix for the perpendicular components of the electric field.

In a similar manner, we can derive the transformation matrix for the parallel components of the electric fields, which is given by

$$\begin{bmatrix} E_{\parallel}^{1\ominus} \\ E_{\parallel}^{1\ominus} \end{bmatrix} = [T]_{\parallel}^E \begin{bmatrix} E_{\parallel}^{2\ominus} \\ E_{\parallel}^{2\ominus} \end{bmatrix} \quad (12)$$

where

$$[T]_{\perp}^E = \begin{bmatrix} \frac{\sqrt{\frac{\epsilon_2}{\mu_2}} \cos \theta_1 + \sqrt{\frac{\epsilon_1}{\mu_1}} \cos \theta_2}{2 \sqrt{\frac{\epsilon_1}{\mu_1}} \cos \theta_1} e^{-j r_2 d_2 - j r_1 d_1}, \frac{\sqrt{\frac{\epsilon_2}{\mu_2}} \cos \theta_1 - \sqrt{\frac{\epsilon_1}{\mu_1}} \cos \theta_2}{2 \sqrt{\frac{\epsilon_1}{\mu_1}} \cos \theta_1} e^{j r_2 d_2 - j r_1 d_1} \\ \frac{\sqrt{\frac{\epsilon_2}{\mu_2}} \cos \theta_1 - \sqrt{\frac{\epsilon_1}{\mu_1}} \cos \theta_2}{2 \sqrt{\frac{\epsilon_1}{\mu_1}} \cos \theta_1} e^{-j r_2 d_2 + j r_1 d_1}, \frac{\sqrt{\frac{\epsilon_2}{\mu_2}} \cos \theta_1 + \sqrt{\frac{\epsilon_1}{\mu_1}} \cos \theta_2}{2 \sqrt{\frac{\epsilon_1}{\mu_1}} \cos \theta_1} e^{j r_2 d_2 + j r_1 d_1} \end{bmatrix} \quad (13)$$

These matrices $[T]_{\perp}^E$ and $[T]_{\parallel}^E$ are used to calculate the coupling between two magnetic dipoles. For the coupling between two electric dipoles, it is necessary to find the transformation matrices for the magnetic field, namely, $[T]_{\perp}^H$ and $[T]_{\parallel}^H$. It is evident that Fig. 1(a) also describes the propagation for the parallel components of the magnetic fields, and Fig. 1(b) the perpendicular components of the magnetic fields. With Eq. (4) and E replaced by H in Eq. (3), it is not difficult to show that the transformation matrices for magnetic fields are given by

$$\begin{bmatrix} H_{\perp}^{1\oplus} \\ H_{\perp}^{1\ominus} \end{bmatrix} = [T]_{\perp}^H \begin{bmatrix} H_{\perp}^{2\oplus} \\ H_{\perp}^{2\ominus} \end{bmatrix} \quad (14)$$

and

$$\begin{bmatrix} H_{\parallel}^{1\oplus} \\ H_{\parallel}^{1\ominus} \end{bmatrix} = [T]_{\parallel}^H \begin{bmatrix} H_{\parallel}^{2\oplus} \\ H_{\parallel}^{2\ominus} \end{bmatrix} \quad (15)$$

where

$$[T]_{\perp}^H = \begin{bmatrix} \frac{\sqrt{\frac{\mu_1}{\epsilon_1}} \cos \theta_1 + \sqrt{\frac{\mu_2}{\epsilon_2}} \cos \theta_2}{2 \sqrt{\frac{\mu_1}{\epsilon_1}} \cos \theta_1} e^{-j r_2 d_2 - j r_1 d_1}, & \frac{\sqrt{\frac{\mu_1}{\epsilon_1}} \cos \theta_1 - \sqrt{\frac{\mu_2}{\epsilon_2}} \cos \theta_2}{2 \sqrt{\frac{\mu_1}{\epsilon_1}} \cos \theta_1} e^{j r_2 d_2 - j r_1 d_1} \\ \frac{\sqrt{\frac{\mu_1}{\epsilon_1}} \cos \theta_1 - \sqrt{\frac{\mu_2}{\epsilon_2}} \cos \theta_2}{2 \sqrt{\frac{\mu_1}{\epsilon_1}} \cos \theta_1} e^{-j r_2 d_2 + j r_1 d_1}, & \frac{\sqrt{\frac{\mu_1}{\epsilon_1}} \cos \theta_1 + \sqrt{\frac{\mu_2}{\epsilon_2}} \cos \theta_2}{2 \sqrt{\frac{\mu_1}{\epsilon_1}} \cos \theta_1} e^{j r_2 d_2 + j r_1 d_1} \end{bmatrix} \quad (16)$$

and

$$[T]_{\parallel}^H = \begin{bmatrix} \frac{\sqrt{\frac{\mu_2}{\epsilon_2}} \cos \theta_1 + \sqrt{\frac{\mu_1}{\epsilon_1}} \cos \theta_2}{2 \sqrt{\frac{\epsilon_1}{\mu_1}} \cos \theta_1} e^{-j r_2 d_2 - j r_1 d_1}, & \frac{\sqrt{\frac{\mu_2}{\epsilon_2}} \cos \theta_1 - \sqrt{\frac{\mu_1}{\epsilon_1}} \cos \theta_2}{2 \sqrt{\frac{\epsilon_1}{\mu_1}} \cos \theta_1} e^{j r_2 d_2 - j r_1 d_1} \\ \frac{\sqrt{\frac{\mu_2}{\epsilon_2}} \cos \theta_1 - \sqrt{\frac{\mu_1}{\epsilon_1}} \cos \theta_2}{2 \sqrt{\frac{\epsilon_1}{\mu_1}} \cos \theta_1} e^{-j r_2 d_2 + j r_1 d_1}, & \frac{\sqrt{\frac{\mu_2}{\epsilon_2}} \cos \theta_1 + \sqrt{\frac{\mu_1}{\epsilon_1}} \cos \theta_2}{2 \sqrt{\frac{\epsilon_1}{\mu_1}} \cos \theta_1} e^{j r_2 d_2 + j r_1 d_1} \end{bmatrix} \quad (17)$$

The matrices $[T]_{\perp}^H$ and $[T]_{\parallel}^H$ can be identified as the transformation matrices for the perpendicular and the parallel components of the magnetic fields, respectively.

Having derived the matrices for a single interface between two dissimilar media, we now proceed to generalize the analysis for the case of multilayered media. Suppose we have n different media and $(n - 1)$ boundaries as shown in Fig. 2. From the preceding results, we have

$$\begin{aligned}
 \begin{bmatrix} W^{1\oplus} \\ W^{1\ominus} \end{bmatrix} &= [T]_{1,2} \begin{bmatrix} W^{2\oplus} \\ W^{2\ominus} \end{bmatrix} \\
 \begin{bmatrix} W^{2\oplus} \\ W^{2\ominus} \end{bmatrix} &= [T]_{2,3} \begin{bmatrix} W^{3\oplus} \\ W^{3\ominus} \end{bmatrix} \\
 &\vdots \\
 \begin{bmatrix} W^{(i-1)\oplus} \\ W^{(i-1)\ominus} \end{bmatrix} &= [T]_{i-1,i} \begin{bmatrix} W^{i\oplus} \\ W^{i\ominus} \end{bmatrix} \\
 &\vdots \\
 \begin{bmatrix} W^{n-1,\oplus} \\ W^{n-1,\ominus} \end{bmatrix} &= [T]_{n-1,n} \begin{bmatrix} W^{n\oplus} \\ W^{n\ominus} \end{bmatrix}
 \end{aligned}$$

where $W^{i\oplus}$ stands for the waves propagating in the $+z$ -direction in the i^{th} medium, and $W^{i\ominus}$ stands for the waves propagating in the $-z$ -direction in the i^{th} medium, i.e.,

$$W^{i\oplus} = E_L^{i\oplus}, E_I^{i\oplus}, H_L^{i\oplus}, \text{ or } H_I^{i\oplus} \quad i = 1, 2, 3, \dots, n$$

$$W^{i\ominus} = E_L^{i\ominus}, E_I^{i\ominus}, H_L^{i\ominus}, \text{ or } H_I^{i\ominus} \quad i = 1, 2, 3, \dots, n$$

We obtain the following results:

$$\begin{bmatrix} W^{1\oplus} \\ W^{1\ominus} \end{bmatrix} = [T]_{1,n} \begin{bmatrix} W^{n\oplus} \\ W^{n\ominus} \end{bmatrix} \quad (18)$$

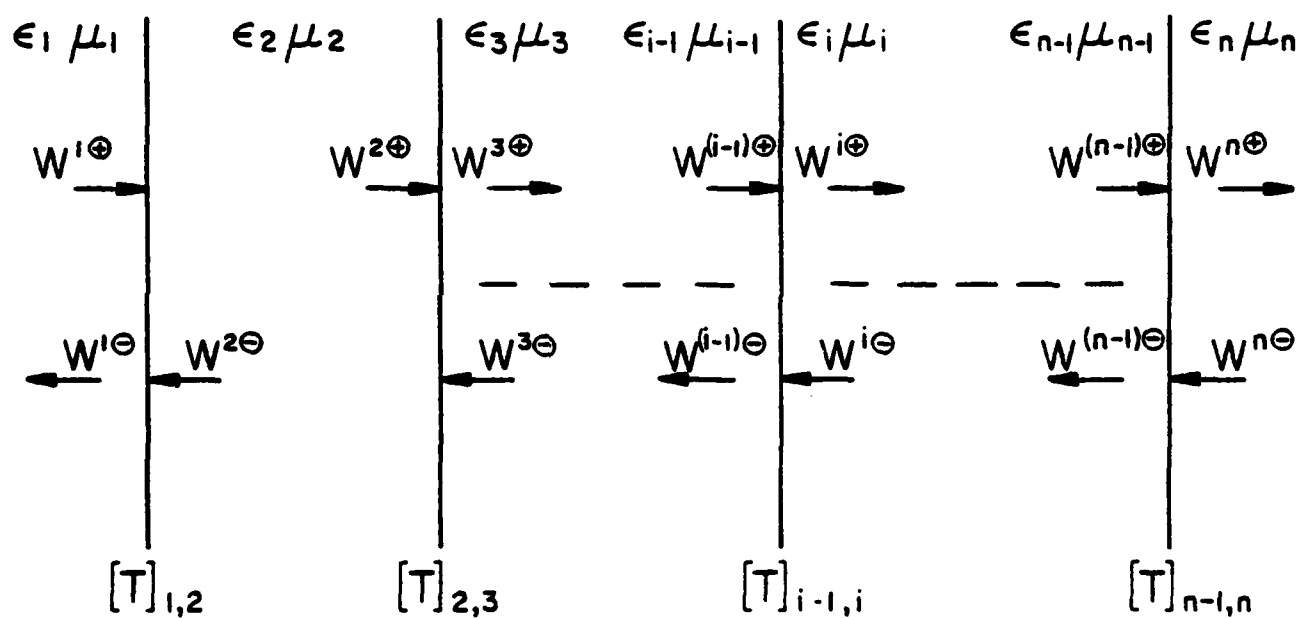


Figure 2. Multilayered media.

where

$$[T]_{1,n} = [T]_{1,2} [T]_{2,3} \dots [T]_{n-1,n} \quad (19)$$

The matrix $[T]_{1,n}$ can be termed the transformation matrix for the N-layer medium.

It is obvious that the transformation matrices only depend on the directions of the waves, the constitutive parameters of the media, and the locations of the terminal planes. For the lossy medium, all of the above formulas are still applicable, provided we replace ϵ by $(\epsilon' + j\epsilon'')$.

3. SPECTRAL REPRESENTATION OF THE RADIATION FIELDS

The fields due to a z-oriented electric dipole located at (x', y', z') can be derived from a z-oriented electric vector potential A_z , which satisfies the equation

$$\nabla^2 A_z + k^2 A_z = -Idl \delta(x - x') \delta(y - y') \delta(z - z') \quad (20)$$

where Idl is the dipole moment of the electric dipole. Equation (20) can be solved via the Fourier transform technique to yield (see Appendix I)

$$A_z(x, y, z) = \frac{Idl}{8\pi^2} \iint_{-\infty}^{\infty} \frac{-j}{\sqrt{k^2 - \alpha^2 - \beta^2}} e^{j[\alpha(x-x') + \beta(y-y') + \gamma(z-z')]} d\alpha d\beta \quad (21)$$

From Maxwell's equation we have

$$\left\{ \begin{array}{l} H_x = \frac{\partial A_z}{\partial y} \\ H_y = -\frac{\partial A_z}{\partial x} \end{array} \right. \quad \left\{ \begin{array}{l} E_x = \frac{1}{j\omega\epsilon} \frac{\partial^2 A_z}{\partial z \partial x} \\ E_y = \frac{1}{j\omega\epsilon} \frac{\partial^2 A_z}{\partial z \partial y} \\ E_z = -j\omega\mu A_z + \frac{1}{j\omega\epsilon} \frac{\partial^2 A_z}{\partial z^2} \end{array} \right. \quad (22)$$

Therefore, the various field components for a z-oriented electric dipole are given as follows

$$\begin{cases}
H_x = \frac{Idl}{8\pi^2} \iint_{-\infty}^{\infty} \frac{\beta}{\sqrt{k^2 - \alpha^2 - \beta^2}} e^{j[\alpha(x-x') + \beta(y-y') + \gamma|z-z'|]} d\alpha d\beta \\
H_y = \frac{Idl}{8\pi^2} \iint_{-\infty}^{\infty} \frac{-\alpha}{\sqrt{k^2 - \alpha^2 - \beta^2}} e^{j[\alpha(x-x') + \beta(y-y') + \gamma|z-z'|]} d\alpha d\beta \\
E_x = \frac{Idl}{8\pi^2} \iint_{-\infty}^{\infty} \frac{-\alpha}{\omega\epsilon} e^{j[\alpha(x-x') + \beta(y-y') + \gamma|z-z'|]} d\alpha d\beta \\
E_y = \frac{Idl}{8\pi^2} \iint_{-\infty}^{\infty} \frac{-\beta}{\omega\epsilon} e^{j[\alpha(x-x') + \beta(y-y') + \gamma|z-z'|]} d\alpha d\beta \\
E_z = \frac{Idl}{8\pi^2} \iint_{-\infty}^{\infty} \frac{-(\alpha^2 + \beta^2)}{\sqrt{k^2 - \alpha^2 - \beta^2}} e^{j[\alpha(x-x') + \beta(y-y') + \gamma|z-z'|]} d\alpha d\beta
\end{cases} \quad (23)$$

where

$$\gamma = \sqrt{k^2 - \alpha^2 - \beta^2}$$

Similarly, we can derive the various field components for an X-oriented electric dipole as follows

$$\begin{cases}
H_y = \frac{Idl}{8\pi^2} \iint_{-\infty}^{\infty} -e^{j[\alpha(x-x') + \beta(y-y') + \gamma|z-z'|]} d\alpha d\beta \\
H_z = \frac{Idl}{8\pi^2} \iint_{-\infty}^{\infty} \frac{-\beta}{\sqrt{k^2 - \alpha^2 - \beta^2}} e^{j[\alpha(x-x') + \beta(y-y') + \gamma|z-z'|]} d\alpha d\beta \\
E_x = \frac{Idl}{8\pi^2} \iint_{-\infty}^{\infty} \frac{-(k^2 - \alpha^2)}{\omega\epsilon\sqrt{k^2 - \alpha^2 - \beta^2}} e^{j[\alpha(x-x') + \beta(y-y') + \gamma|z-z'|]} d\alpha d\beta \\
E_y = \frac{Idl}{8\pi^2} \iint_{-\infty}^{\infty} \frac{\alpha\beta}{\omega\epsilon\sqrt{k^2 - \alpha^2 - \beta^2}} e^{j[\alpha(x-x') + \beta(y-y') + \gamma|z-z'|]} d\alpha d\beta \\
E_z = \frac{Idl}{8\pi^2} \iint_{-\infty}^{\infty} \frac{-\alpha}{\omega\epsilon} e^{j[\alpha(x-x') + \beta(y-y') + \gamma|z-z'|]} d\alpha d\beta
\end{cases} \quad (24)$$

From duality, we know that

$$\begin{cases} \overline{\mathbf{E}} \rightarrow \overline{\mathbf{H}} \\ \overline{\mathbf{H}} \rightarrow -\overline{\mathbf{E}} \end{cases} \begin{cases} \mathbf{Idl} \rightarrow kdl \\ kdl \rightarrow \mathbf{Idl} \end{cases} \begin{cases} \epsilon \rightarrow \mu \\ \mu \rightarrow \epsilon \end{cases} \quad (25)$$

where kdl is the dipole moment of the magnetic dipole. Consequently, the various field components for the magnetic dipole can be obtained directly from those of the electric dipole upon application of the duality principle.

The various field components for the z-oriented magnetic dipole are

$$\left\{ \begin{aligned} E_x &= \frac{kdl}{8\pi^2} \iint_{-\infty}^{\infty} \frac{-\beta}{\sqrt{k^2 - \alpha^2 - \beta^2}} e^{j[\alpha(x-x') + \beta(y-y') + \gamma|z-z'|]} d\alpha d\beta \\ E_y &= \frac{kdl}{8\pi^2} \iint_{-\infty}^{\infty} \frac{\alpha}{\sqrt{k^2 - \alpha^2 - \beta^2}} e^{j[\alpha(x-x') + \beta(y-y') + \gamma|z-z'|]} d\alpha d\beta \\ H_x &= \frac{kdl}{8\pi^2} \iint_{-\infty}^{\infty} \frac{-\alpha}{\omega\mu} e^{j[\alpha(x-x') + \beta(y-y') + \gamma|z-z'|]} d\alpha d\beta \\ H_y &= \frac{kdl}{8\pi^2} \iint_{-\infty}^{\infty} \frac{-\beta}{\omega\mu} e^{j[\alpha(x-x') + \beta(y-y') + \gamma|z-z'|]} d\alpha d\beta \\ H_z &= \frac{kdl}{8\pi^2} \iint_{-\infty}^{\infty} \frac{-(\alpha^2 + \beta^2)}{\omega\mu\sqrt{k^2 - \alpha^2 - \beta^2}} e^{j[\alpha(x-x') + \beta(y-y') + \gamma|z-z'|]} d\alpha d\beta \end{aligned} \right. \quad (26)$$

Likewise, the components for the x-oriented magnetic dipole are given by

$$\left\{ \begin{aligned}
 E_y &= \frac{k d l}{8 \pi^2} \iint_{-\infty}^{\infty} e^{j[\alpha(x-x')+\beta(y-y')+\gamma|z-z'|]} d\alpha d\beta \\
 E_z &= \frac{k d l}{8 \pi^2} \iint_{-\infty}^{\infty} \frac{\beta}{\sqrt{k^2 - \alpha^2 - \beta^2}} e^{j[\alpha(x-x')+\beta(y-y')+\gamma|z-z'|]} d\alpha d\beta \\
 H_x &= \frac{k d l}{8 \pi^2} \iint_{-\infty}^{\infty} \frac{-j(k^2 - \alpha^2)}{\omega \mu \sqrt{k^2 - \alpha^2 - \beta^2}} e^{j[\alpha(x-x')+\beta(y-y')+\gamma|z-z'|]} d\alpha d\beta \\
 H_y &= \frac{k d l}{8 \pi^2} \iint_{-\infty}^{\infty} \frac{j \alpha \beta}{\omega \mu \sqrt{k^2 - \alpha^2 - \beta^2}} e^{j[\alpha(x-x')+\beta(y-y')+\gamma|z-z'|]} d\alpha d\beta \\
 H_z &= \frac{k d l}{8 \pi^2} \iint_{-\infty}^{\infty} \frac{-j \alpha}{\omega \mu} e^{j[\alpha(x-x')+\beta(y-y')+\gamma|z-z'|]} d\alpha d\beta
 \end{aligned} \right. \quad (27)$$

4. NUMERICAL COMPUTATION

4.1. Collinear Magnetic Dipoles (or Small Coaxial Loops)

Suppose we have two z-oriented collinear magnetic dipoles separated by a shield. Loop 1 is a transmitting antenna placed at the origin of Cartesian coordinates (0,0,0), whereas Loop 2 is a receiving antenna at the point (0,0,z₀), as shown in Figure 3.

Letting the terminal planes at z = 0 and z = z, respectively, the incident electric fields $E_x^{l\oplus}$, $E_y^{l\oplus}$ for the magnetic dipole at the plane 1 are

$$\begin{cases} E_x^{l\oplus}(x,y,0) = \frac{kdl}{8\pi^2} \iint \frac{-\beta}{\sqrt{k^2 - \alpha^2 - \beta^2}} e^{j(\alpha x + \beta y)} d\alpha d\beta \\ E_y^{l\oplus}(x,y,0) = \frac{kdl}{8\pi^2} \iint \frac{\alpha}{\sqrt{k^2 - \alpha^2 - \beta^2}} e^{j(\alpha x + \beta y)} d\alpha d\beta \end{cases} \quad (28)$$

From the matrix Eq. (A.12) in Appendix 2, we obtain

$$\begin{bmatrix} \tilde{E}_x^{l\oplus} \\ \tilde{E}_y^{l\oplus} \end{bmatrix} = \begin{bmatrix} \frac{\beta}{\sqrt{\alpha^2 + \beta^2}}, & -\frac{\alpha}{\sqrt{\alpha^2 + \beta^2}} \\ \frac{\alpha\sqrt{k^2 - \alpha^2 - \beta^2}}{k\sqrt{\alpha^2 + \beta^2}}, & \frac{\beta\sqrt{k^2 - \alpha^2 - \beta^2}}{k\sqrt{\alpha^2 + \beta^2}} \end{bmatrix} \begin{bmatrix} \tilde{E}_x^{l\oplus} \\ \tilde{E}_y^{l\oplus} \end{bmatrix} \quad (29)$$

and

$$\begin{cases} E_x^{l\oplus}(x,y,0) = \frac{kdl}{8\pi^2} \iint_{-\infty}^{\infty} \frac{-\sqrt{\alpha^2 + \beta^2}}{\sqrt{k^2 - \alpha^2 - \beta^2}} e^{j(\alpha x + \beta y)} d\alpha d\beta \\ E_y^{l\oplus}(x,y,0) = 0 \end{cases} \quad (30)$$

This result shows that the direction of every incident electric field at plane 1 is always perpendicular to its plane of incidence, because the electric field of

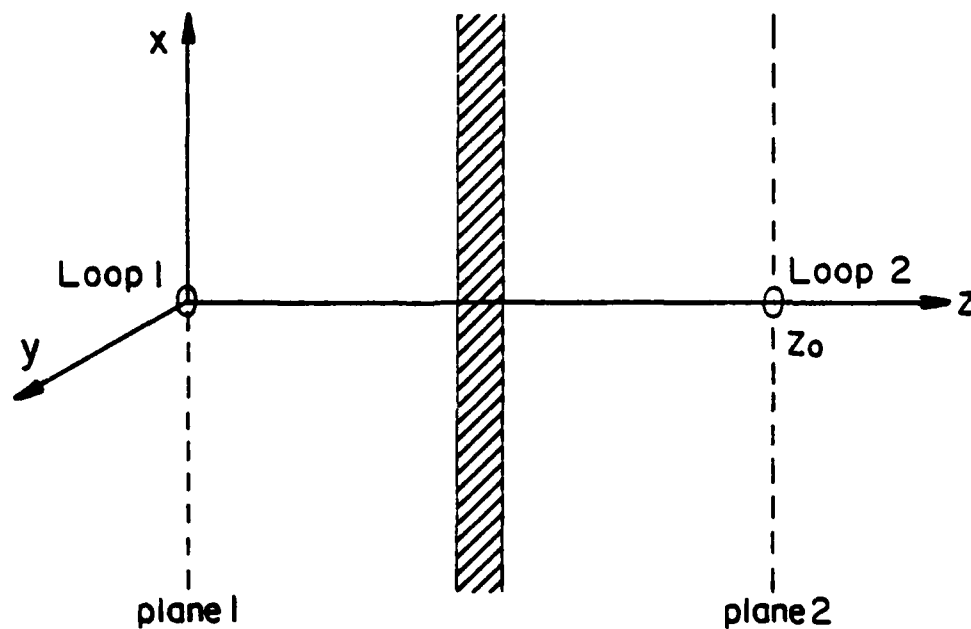


Figure 3. Two coaxial loops separated by a shield.

the z-oriented magnetic dipole in the cylindrical coordinates (ρ, ϕ, z) has the one ϕ -component.

Let

$$\begin{cases} W^{1\oplus} = \tilde{E}_1^{1\oplus} \\ W^{1\ominus} = \tilde{E}_1^{1\ominus} \end{cases} \quad \begin{cases} W^{2\oplus} = \tilde{E}_1^{2\oplus} \\ W^{2\ominus} = 0 \end{cases} \quad (31)$$

Finally,

$$\tilde{E}_1^{1\oplus} = \frac{1}{T_{11}^1} \tilde{E}_1^{1\oplus} \quad (32)$$

where T_{11}^1 is the first element of the matrix $[T]^E$ which is $[T]^E \cdot [T]^E$. The matrix $[T]^E$ is the transformation matrix for the left boundary, whereas the $[T]^E$ is the one for the right.

Therefore, one may obtain the field at plane 2

$$E_1^{2\oplus}(x, y, z_0) = \frac{kdl}{8\pi^2} \iint_{-\infty}^{\infty} \frac{-\sqrt{\alpha^2 + \beta^2}}{T_{11}^1 \sqrt{k^2 - \alpha^2 - \beta^2}} e^{j(\alpha x + \beta y)} d\alpha d\beta \quad (33)$$

In order to find the magnetic fields received by loop 2, it is necessary to transform the $E_1^{2\oplus}$ into the components $E_x^{2\oplus}$ and $E_y^{2\oplus}$. From the matrix Eq. (A.13) in Appendix 2, we obtain

$$\begin{bmatrix} \tilde{E}_x \\ \tilde{E}_y \end{bmatrix} = \begin{bmatrix} \frac{\beta}{\sqrt{\alpha^2 + \beta^2}} & \frac{\alpha k}{\sqrt{\alpha^2 + \beta^2} \sqrt{k^2 - \alpha^2 - \beta^2}} \\ -\frac{\alpha}{\sqrt{\alpha^2 + \beta^2}} & \frac{\beta k}{\sqrt{\alpha^2 + \beta^2} \sqrt{k^2 - \alpha^2 - \beta^2}} \end{bmatrix} \begin{bmatrix} \tilde{E}_1 \\ \tilde{E}_1 \end{bmatrix} \quad (A13)$$

and

$$\begin{cases} E_x^{20}(x, y, z_0) = \frac{k d \ell}{8 \pi^2} \iint_{-\infty}^{\infty} \frac{-\beta}{T_{11}^{\perp} \sqrt{k^2 - \alpha^2 - \beta^2}} e^{j(\alpha x + \beta y)} d\alpha d\beta \\ E_y^{20}(x, y, z_0) = \frac{k d \ell}{8 \pi^2} \iint_{-\infty}^{\infty} \frac{\alpha}{T_{11}^{\perp} \sqrt{k^2 - \alpha^2 - \beta^2}} e^{j(\alpha x + \beta y)} d\alpha d\beta \end{cases} \quad (34)$$

It is obvious that the z-oriented magnetic dipole placed at the z-axis can only couple the z-component of the magnetic field. From Maxwell's equation we have

$$H_z = j \frac{1}{\omega \mu} \left[\frac{\partial E_y}{\partial x} - \frac{\partial E_x}{\partial y} \right] \quad (35)$$

and

$$H_z(x, y, z_0) = \frac{1}{8 \pi^2 \omega \mu} \iint_{-\infty}^{\infty} \frac{-(\alpha^2 + \beta^2)}{T_{11}^{\perp} \sqrt{k^2 - \alpha^2 - \beta^2}} e^{j(\alpha x + \beta y)} d\alpha d\beta \quad (36)$$

In order to evaluate this integral, let us make the following substitutions [2]:

$$\begin{cases} \alpha = \lambda \cos \xi \\ \beta = \lambda \sin \xi \end{cases} \quad \begin{cases} x = \rho \cos \phi \\ y = \rho \sin \phi \end{cases} \quad (37)$$

It is worth noting that the first element T_{11}^{\perp} of the matrix $[T]^E$ is only a function of λ and independent of ξ , because the factors contained in the matrix become

$$\begin{aligned} \cos \theta &= \frac{\sqrt{k^2 - \alpha^2 - \beta^2}}{k} = \frac{\sqrt{k^2 - \lambda^2}}{k} \\ \gamma &= \sqrt{k^2 - \alpha^2 - \beta^2} = \sqrt{k^2 - \lambda^2} \end{aligned} \quad (38)$$

Hence, one can separate the above double integral and obtain

$$\begin{aligned}
H_z(\rho, \phi, z_0) &= \frac{1}{8\pi^2 \omega \mu} \int_0^\infty \frac{-\lambda^3 d\lambda}{T_{11}^1 \sqrt{k^2 - \lambda^2}} \int_{-\pi}^{\pi} e^{j\rho\lambda \cos(\xi - \phi)} d\xi \\
&= \frac{1}{8\pi^2 \omega \mu} \int_0^\infty \frac{-2\pi\lambda^3}{T_{11}^1 \sqrt{k^2 - \lambda^2}} J_0(\rho\lambda) d\lambda
\end{aligned} \tag{39}$$

Making another substitution

$$\lambda = k \sin \zeta \tag{40}$$

we have

$$H_z(\rho, \phi, z_0) = \frac{k d l}{8\pi^2 \omega \mu c} \int \frac{-2\pi k^3 \sin^3 \zeta}{T_{11}^1} \cdot J_0(k\rho \sin \zeta) d\zeta \tag{41}$$

where c is a contour in the complex ζ -plane, as specified by the transformation $\lambda = k \sin \zeta$. In this case, the magnetic dipole is placed in the free space, so k is real. Let $k = k'$. Then

$$\lambda = \lambda' + j\lambda'' = k'[\sin \zeta' \operatorname{ch} \zeta'' + j \cos \zeta' \operatorname{sh} \zeta''] \tag{42}$$

It is easy to show that the mapping of Eq. (34) transforms the quadrants of the λ -plane into parallel strips of width $\pi/2$ radians. The path of the integrands in Eq. (39), that runs from $\lambda = 0$ to $\lambda = +\infty$ in the right-half plane, is now transformed into the path c , as shown in Fig. 4.

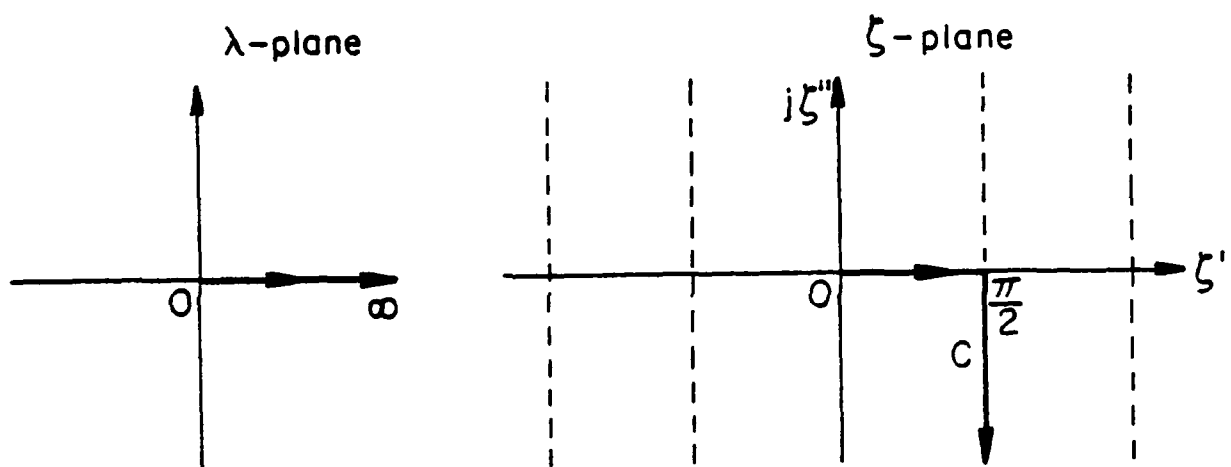


Figure 4. Contour transformation.

Finally, we have

$$H_z(\rho, \phi, z_0) = \frac{-k^3 k d l}{4 \pi \omega \mu} \left[\int_0^{\frac{\pi}{2}} \frac{\sin^3 d \zeta'}{T_{11}^1(\cos \zeta')} \cdot J_0(k \rho \sin \zeta') d \zeta' - \int_{-\infty}^{\infty} \frac{\text{ch}^3 \zeta''}{T_{11}^1(\text{sh} \zeta'')} J_0(k \rho \text{ch} \zeta'') d \zeta'' \right] \quad (43)$$

The magnetic field received from the z-oriented magnetic dipole placed along the z-axis is

$$H_z(0, 0, z_0) = \frac{-k^3 k d l}{4 \pi \omega \mu} \left[\int_0^{\frac{\pi}{2}} \frac{\sin^3 d \zeta'}{T_{11}^1(\cos \zeta')} d \zeta' - \int_{-\infty}^{\infty} \frac{\text{ch}^3 \zeta''}{T_{11}^1(\text{sh} \zeta'')} d \zeta'' \right] \quad (44)$$

If the shield is removed, it becomes a free space. From Eqs. (26), the component of the magnetic field on plane 2 is obtained

$$H_{z_0}(x, y, z_0) = \frac{k d l}{8 \pi^2 \omega \mu} \iint_{-\infty}^{\infty} \frac{-(\alpha^2 + \beta^2)}{\sqrt{k^2 - \alpha^2 - \beta^2}} e^{j(\alpha x + \beta y)} e^{j \sqrt{k^2 - \alpha^2 - \beta^2} z_0} d \alpha d \beta \quad (45)$$

Using the same substitutions in Eqs. (37) and (40), one may obtain

$$H_{z_0}(\rho, \phi, z_0) = \frac{-k^3 k d l}{4 \pi \omega \mu} \left[\int_0^{\frac{\pi}{2}} \sin^3 \zeta' J_0(k \rho \sin \zeta') e^{j k z_0 \cos \zeta'} d \zeta' + \int_0^{-\infty} \text{ch}^3 \zeta'' J_0(k \rho \text{ch} \zeta'') e^{k z_0 \text{sh} \zeta''} d \zeta'' \right] \quad (46)$$

and

$$H_{z_0}(0, 0, z) = \frac{-k^3 k d l}{4 \pi \omega \mu} \left[\int_0^{\frac{\pi}{2}} \sin^3 \zeta' e^{j k z_0 \cos \zeta'} d \zeta' - \int_0^{-\infty} \text{ch}^3 \zeta'' e^{k z_0 \text{sh} \zeta''} d \zeta'' \right] \quad (47)$$

Let us define the shielding coefficient of the shield as

$$S_H = 20 \log \frac{|H_{z0}(0,0,z_0)|(\text{free space})}{|H_z(0,0,z_0)|(\text{with shield})} \text{ (db)} \quad (48)$$

It can be used to describe the coupling between two coaxial z-oriented small loops separated by the shield. The large S means that the coupling is weak.

4.2. Collinear Electric Dipole

Consider two z-oriented collinear electric dipoles separated by a shield, as shown in Fig. 5. Invoking duality (Eq. (25)), it is possible to find the z-component of the electric field at plane 2 directly

$$E_z(\rho, \phi, z_0) = \frac{-k^2 Id\ell}{4\pi^2 \omega \epsilon} \left[\int_0^{\frac{\pi}{2}} \frac{\sin^3 d\zeta'}{T_{11}^1(\cos \zeta')} \cdot J_0(k\rho \sin \zeta') d\zeta' - \int_{-\infty}^{\infty} \frac{\text{ch}^3 \zeta''}{T_{11}^1(\text{sh} \zeta'')} J_0(k\rho \text{ch} \zeta'') d\zeta'' \right] \quad (49)$$

and

$$E_z(0,0,z_0) = \frac{k^3 Id\ell}{4\pi^2 \omega \epsilon} \left[\int_0^{\frac{\pi}{2}} \frac{\sin^3 d\zeta'}{T_{11}^1(\cos \zeta')} d\zeta' - \int_{-\infty}^{\infty} \frac{\text{ch}^3 \zeta''}{T_{11}^1(\text{sh} \zeta'')} d\zeta'' \right] \quad (50)$$

But T_{11}^1 is the first element of the transformation matrix for the perpendicular component of the magnetic fields $[T]_{\perp}^H$ in Eq. (15), instead of $[T]_{\perp}^E$.

For free space, we have

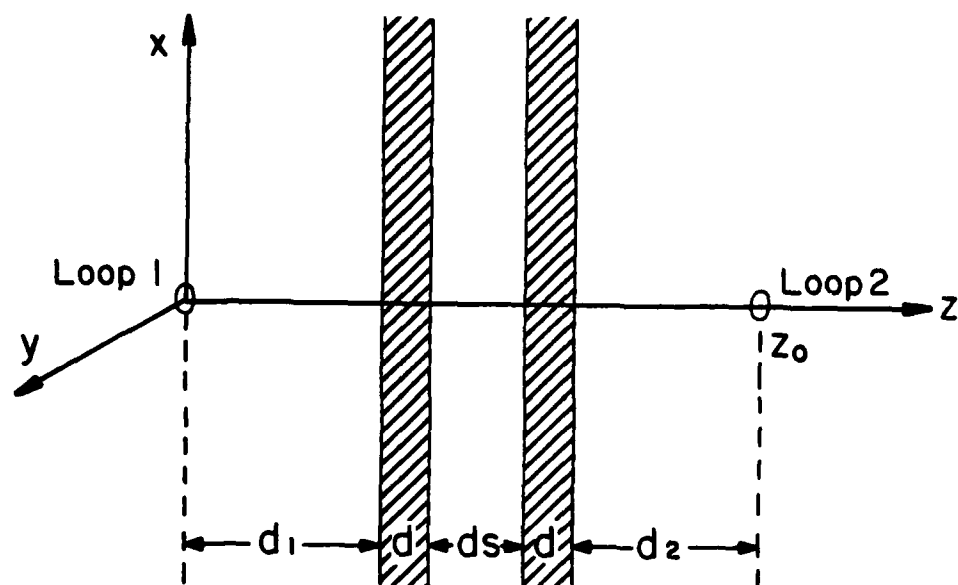


Figure 5. Two coaxial loops separated by a double copper shield.

$$E_z(0,0,z_0) = \frac{-k^3 Idl}{4\pi\omega\epsilon} \left[\int_0^{\frac{\pi}{2}} \sin^3 \zeta' e^{jkz_0 \cos \zeta'} d\zeta' - \int_0^{-\infty} \operatorname{ch}^3 \zeta'' e^{kz_0 \operatorname{sh} \zeta''} d\zeta'' \right] \quad (51)$$

Similarly, we can define the shielding coefficient of the shield as

$$S_E = 20 \log \frac{|E_{z_0}(0,0,z_0)|(\text{free space})}{|E_z(0,0,z_0)|(\text{with shield})} \quad (\text{dB}) \quad (52)$$

It describes the coupling between two collinear electric dipoles separated by a shield.

5. NUMERICAL RESULTS

We have two coaxial loops separated by a double copper shield. Let us compute the shielding coefficient of this shield. The thickness of each shield is $(1/1000)''$; the separation between the two shields is $ds = (1/2)''$ or $(1/8)''$; and the distances from the dipoles to the shields are $d_1 = d_2 = 12''$, as shown in Fig. 5.

The variations of the shielding coefficient with frequency for magnetic dipoles, electric dipoles, and plane waves are shown in Fig. 6. Experimental results for magnetic dipoles are also given. From these results, we know that the copper shield, which has a very high electric conductivity, possesses a higher shielding coefficient for electric dipoles.

It is worth noting that in the above calculation we have assumed that the propagation direction of each of the components radiated by the dipole is always perpendicular to the boundaries in the double copper shield (see Fig. 7). This is because the electrical conductivity of copper is very high.

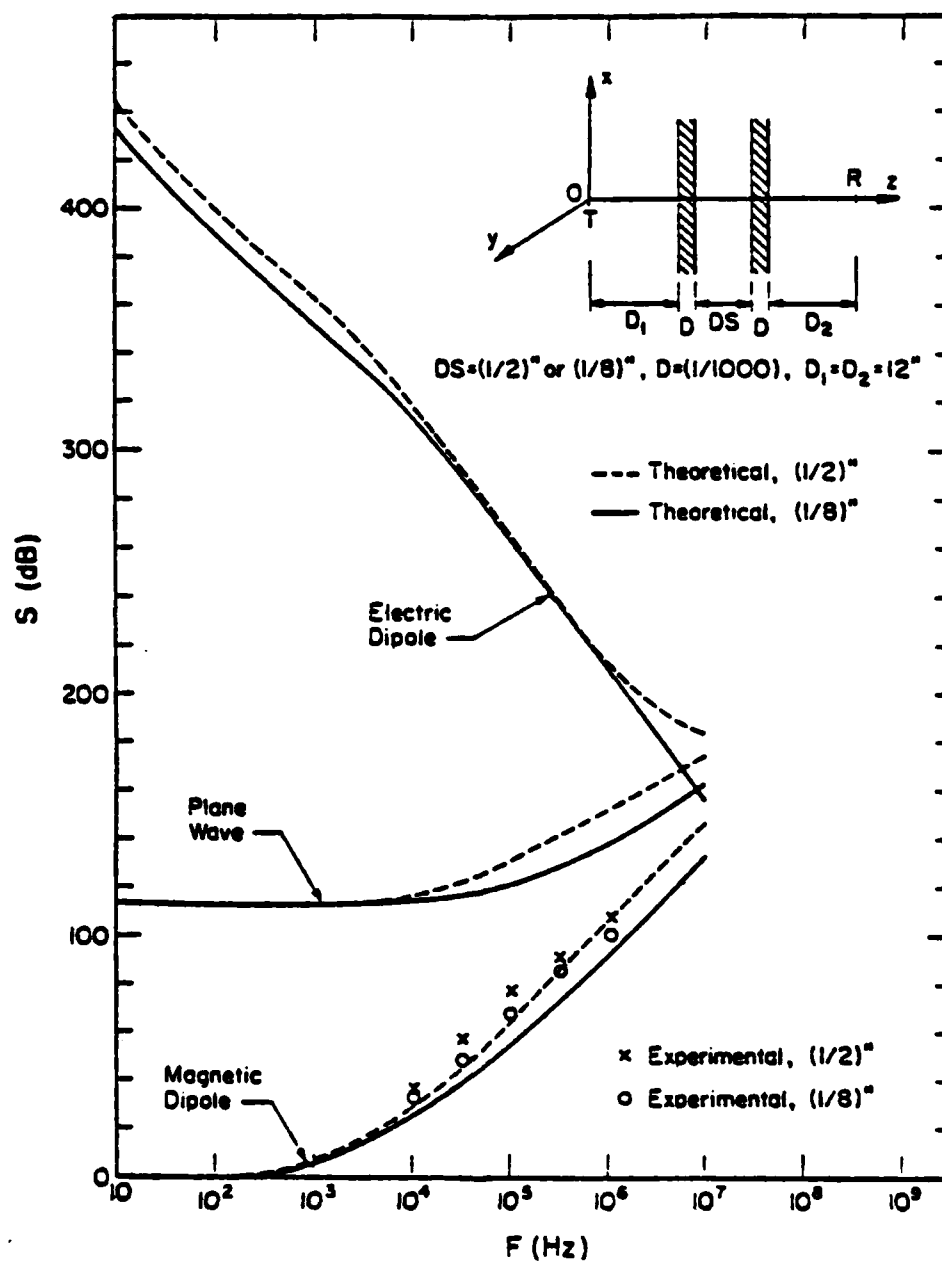


Figure 6. Theoretical and experimental results for electric dipoles, plane wave and magnetic dipoles.

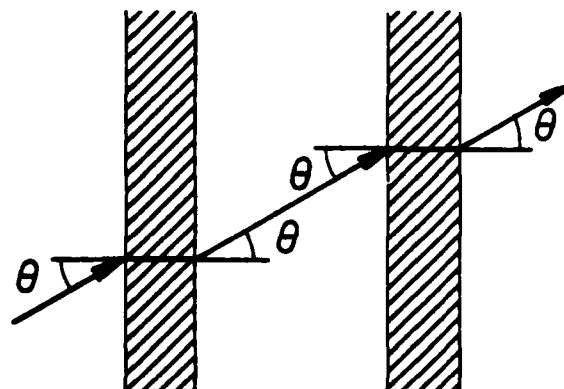


Figure 7. The propagation direction of each of the components radiated by the dipole.

6. CONCLUSION

The formulas given in References [3] and [4] are only for specially oriented dipoles, i.e., the dipoles must be perpendicular to the boundary. The formulas are not available for arbitrarily oriented dipoles. We have already obtained formulas for z-oriented and x-oriented dipoles. The former is perpendicular to the boundary, whereas the latter is parallel. If a dipole is oriented in an arbitrary direction to the boundary, we can always resolve the dipole into two equivalent dipoles. One is z-oriented, and the other is x-oriented. Therefore, the above approach can be used for arbitrarily oriented dipoles. Furthermore, the boundary transformation matrices obtained in this paper are also useful for the study of wave propagation in stratified media. The method presented in this paper is simple and convenient.

APPENDIX 1

FIELD EQUATIONS

We have

$$\nabla^2 A_z + k A_z = -Id\ell \delta(x-x') \delta(y-y') \delta(z-z') \quad (A.1)$$

Let

$$A_z(x,y,z) = \iiint_{-\infty}^{\infty} \tilde{A}_z(\alpha, \beta, \gamma) e^{j[\alpha(x-x') + \beta(y-y') + \gamma(z-z')] } d\alpha d\beta d\gamma \quad (A.2)$$

Fourier transforming Eq. (A.1) we get

$$(k^2 - (\alpha^2 + \beta^2 + \gamma^2)) \tilde{A}_z(\alpha, \beta, \gamma) = -\frac{Id\ell}{(2\pi)^3}$$

Therefore,

$$\tilde{A}_z(\alpha, \beta, \gamma) = -\frac{Id\ell}{(2\pi)^3(k^2 - (\alpha^2 + \beta^2 + \gamma^2))}$$

Thus the solution of Eq. (A.1) is

$$\begin{aligned} A_z(x,y,z) &= -\frac{Id\ell}{8\pi^3} \iiint_{-\infty}^{\infty} e^{j[\alpha(x-x') + \beta(y-y')] } d\alpha d\beta d\gamma \\ &= -\frac{Id\ell}{8\pi^3} \iint_{-\infty}^{\infty} e^{j[\alpha(x-x') + \beta(y-y')] } d\alpha d\beta \int_{-\infty}^{\infty} \frac{e^{j\gamma(z-z')}}{(k^2 - \alpha^2 - \beta^2) - \gamma^2} d\gamma \end{aligned} \quad (A.3)$$

Let $k^2 - \alpha^2 - \beta^2 = K^2$, and $K = \sqrt{k^2 - \alpha^2 - \beta^2}$. Then the second integral of Eq. (A.3) becomes

$$\int_{-\infty}^{\infty} \frac{e^{j\gamma(z-z')}}{K^2 - \gamma^2} d\gamma \quad (A.4)$$

Applying the complex function theory to evaluate this integration, it is evident that the integrand $\frac{e^{j\gamma(z-z')}}{K^2 - \gamma^2}$ has two poles $\gamma = \pm K$ on the real axis in

the complex γ -plane. From the radiation condition, we know that only one pole is reasonable and that

$$\gamma = R(\cos \phi + j \sin \phi)$$

Therefore,

$$|e^{j\gamma(z-z')}| = e^{-R(z-z') \sin \phi} \quad (\text{A.5})$$

Since $\sin \phi > 0$ in the upper-half plane, the integrand will become negligibly small as R increases without bound, but only if $z > z'$. Thus, we can take the contour as shown in Fig. A.1. For $z > z'$, the contour includes only one pole ($r = +K$). We then obtain in the limit

$$\begin{aligned} \int_{-\infty}^{\infty} \frac{e^{j\gamma(z-z')}}{K^2 - \gamma^2} d\gamma &= 2\pi j \operatorname{Res} \left[\frac{e^{j\gamma(z-z')}}{K^2 - \gamma^2} \right]_{\gamma = \pm K} \\ &= \frac{j\pi e^{jK(z-z')}}{K} = \frac{j\pi e^{j\sqrt{k^2 - \alpha^2 - \beta^2}(z-z')}}{\sqrt{k^2 - \alpha^2 - \beta^2}} \quad (z > z') \end{aligned} \quad (\text{A.6})$$

Obviously, for $z < z'$ the contour must be closed in the lower-half plane, as shown in Fig. A.2. The contour includes another pole ($\gamma = -K$), so that

$$\begin{aligned} \int_{-\infty}^{\infty} \frac{e^{j\gamma(z-z')}}{K^2 - \gamma^2} d\gamma &= -2\pi j \operatorname{Res} \frac{e^{-j\gamma(z-z')}}{K^2 - \gamma^2} \\ &= \frac{j\pi e^{-j\sqrt{k^2 - \alpha^2 - \beta^2}(z-z')}}{\sqrt{k^2 - \alpha^2 - \beta^2}} \quad (z < z') \end{aligned} \quad (\text{A.7})$$

and for $z > z'$ or $z < z'$

$$\int_{-\infty}^{\infty} \frac{e^{j\gamma(z-z')}}{K^2 - \gamma^2} d\gamma = \frac{j\pi e^{j\sqrt{k^2 - \alpha^2 - \beta^2}|z-z'|}}{\sqrt{k^2 - \alpha^2 - \beta^2}} \begin{cases} z > z' \\ \text{or } z < z' \end{cases} \quad (\text{A.8})$$

Finally, we have

$$A(x, y, z) = -\frac{Idl}{8\pi^3} \iint_{-\infty}^{\infty} \frac{j}{\sqrt{k^2 - \alpha^2 - \beta^2}} e^{j[\alpha(x-x') + \beta(y-y') + \sqrt{k^2 - \alpha^2 - \beta^2}|z-z'|]} d\alpha d\beta \quad (\text{A.9})$$

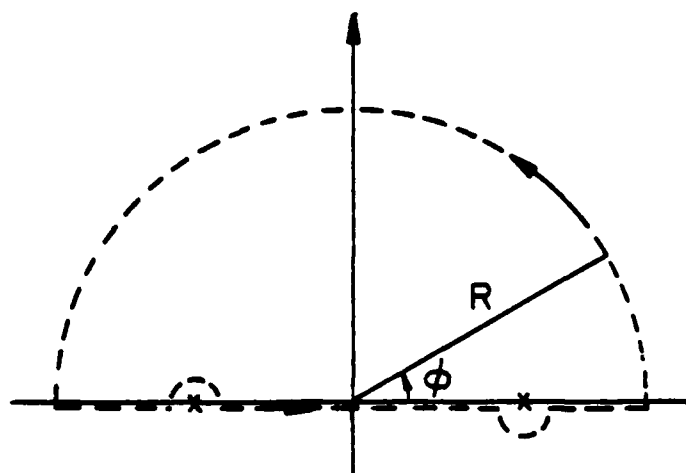


Figure A.1. Contour for $z > z'$.

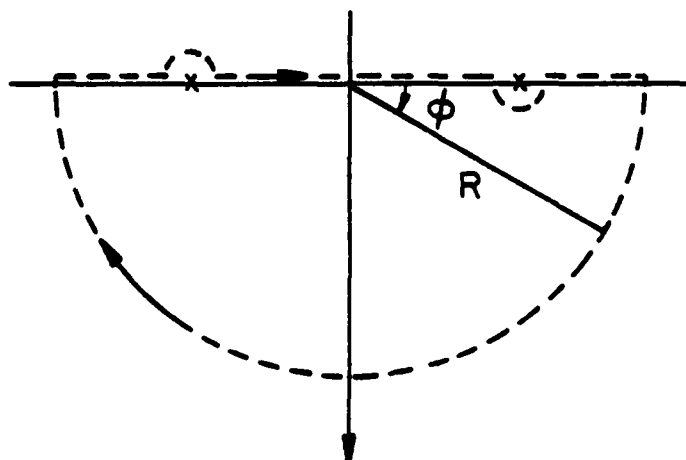


Figure A.2. Contour for $z < z'$.

APPENDIX 2

COORDINATE TRANSFORMATION

Considering the coordinate transformation from the $\overline{E}_x, \overline{E}_y, \overline{E}_z$ coordinate system to the system defined by the orthogonal triad consisting of the wave vector \overline{k} and vectors \overline{E}_\parallel and \overline{E}_\perp shown in Fig. A.3, we obtain a coordinate transformation matrix

$$\begin{bmatrix} \overline{E}_\perp \\ \overline{E}_\parallel \\ \overline{k} \end{bmatrix} = [R] \begin{bmatrix} \overline{E}_x \\ \overline{E}_y \\ \overline{E}_z \end{bmatrix} \quad (\text{A.10})$$

where

$$[R] = \begin{bmatrix} \sin \phi & -\cos \phi & 0 \\ \cos \phi \cos \theta & \sin \phi \cos \theta & -\sin \theta \end{bmatrix} \quad (\text{A.11})$$

The final results are

$$\begin{bmatrix} \overline{E}_\perp \\ \overline{E}_\parallel \end{bmatrix} = \begin{bmatrix} \sin \phi & -\cos \phi \\ \cos \phi \cos \theta & \sin \phi \cos \theta \end{bmatrix} \begin{bmatrix} E_x \\ E_y \end{bmatrix} \quad (\text{A.12})$$

$$\begin{bmatrix} E_x \\ E_y \end{bmatrix} = \begin{bmatrix} \sin \phi & \frac{\cos \phi}{\cos \theta} \\ -\cos \phi & \frac{\sin \phi}{\cos \theta} \end{bmatrix} \begin{bmatrix} \overline{E}_\perp \\ \overline{E}_\parallel \end{bmatrix} \quad (\text{A.13})$$

and

$$\begin{bmatrix} \overline{E}_\perp \\ \overline{E}_\parallel \end{bmatrix} = \begin{bmatrix} -\cos \phi & 0 \\ \sin \phi \cos \theta & -\sin \theta \end{bmatrix} \begin{bmatrix} \overline{E}_y \\ \overline{E}_z \end{bmatrix} \quad (\text{A.14})$$

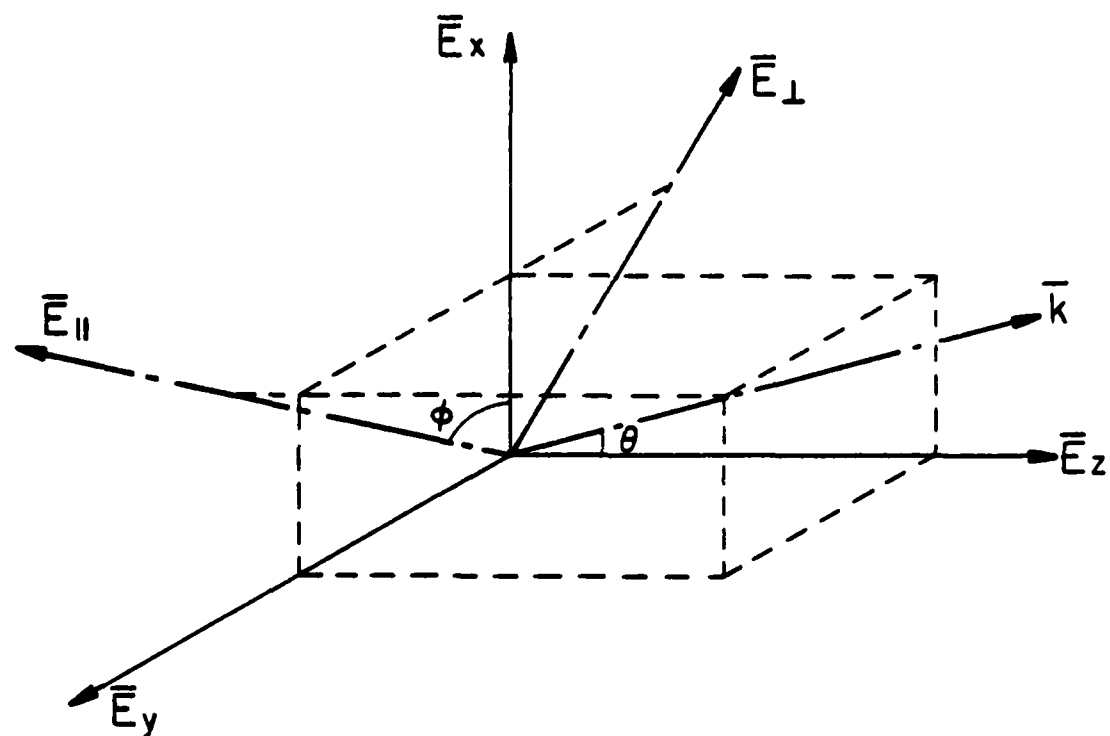


Figure A.3. Coordinate transformation.

$$\begin{bmatrix} \overline{E}_y \\ - \\ \overline{E}_z \end{bmatrix} = \begin{bmatrix} -\frac{1}{\cos \phi} & \\ \sin \phi \cos \theta & \\ -\frac{1}{\cos \phi \sin \theta} & \frac{1}{\sin \theta} \end{bmatrix} \begin{bmatrix} \overline{E}_\perp \\ \\ \overline{E}_\parallel \end{bmatrix} \quad (\text{A.15})$$

where

$$\begin{cases} \cos \theta = \frac{\overline{\mathbf{k}} \cdot \hat{\mathbf{z}}}{|\overline{\mathbf{k}}|} = \frac{\sqrt{k^2 - \alpha^2 - \beta^2}}{k} ; & \sin \theta = \frac{\sqrt{\alpha^2 - \beta^2}}{k} \\ \cos \phi = \frac{\overline{\mathbf{k}} \cdot \hat{\mathbf{x}}}{\sqrt{|\overline{\mathbf{k}}|^2 - (\overline{\mathbf{k}} \cdot \hat{\mathbf{z}})^2}} = \frac{\alpha}{\sqrt{\alpha^2 + \beta^2}} ; & \sin \phi = \frac{\beta}{\sqrt{\alpha^2 + \beta^2}} \end{cases} \quad (\text{A.16})$$

REFERENCES

- [1] P.C. Clemmow, The Plane Wave Spectrum Representation in Electromagnetic Fields. London: Pergamon Press, 1966.
- [2] G. Tyras, Radiation and Propagation of Electromagnetic Waves. New York: Academic Press, 1969.
- [3] J. R. Moser, "Low-Frequency Shielding of a Circular Loop Electromagnetic Field Source," IEEE Transactions on Electromagnetic Compatibility, vol. EMC-9, no. 1, March 1967.
- [4] P. R. Bannister, "Further Notes for Predicting Shielding Effectiveness for the Plane Shield Case," IEEE Transactions on Electromagnetic Compatibility, vol. EMC-11, no. 2, May 1969.

FILMED

02 - 84